

PROGRESS REPORT FOR AFOARD FUNDED PROJECT #FA5209-05-P0063  
titled:

Development of Gallium Arsenide based NEMS processing for investigation of  
energy loss mechanisms in resonators

PI: Yun Daniel Park, Assistant Professor of Physics  
CSCMR & School of Physics  
Seoul National University  
Seoul 151-747 Korea

Contractor:  
Seoul National University  
San 56-1 Silim-dong Gwanak-gu  
Seoul 151-742 Korea

---

# Report Documentation Page

*Form Approved  
OMB No. 0704-0188*

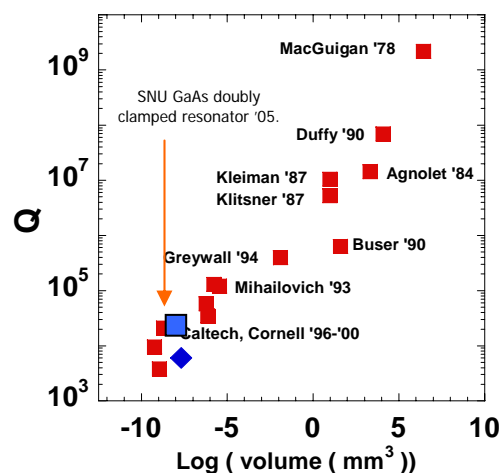
Public reporting burden for the collection of information is estimated to average 1 hour per response, including the time for reviewing instructions, searching existing data sources, gathering and maintaining the data needed, and completing and reviewing the collection of information. Send comments regarding this burden estimate or any other aspect of this collection of information, including suggestions for reducing this burden, to Washington Headquarters Services, Directorate for Information Operations and Reports, 1215 Jefferson Davis Highway, Suite 1204, Arlington VA 22202-4302. Respondents should be aware that notwithstanding any other provision of law, no person shall be subject to a penalty for failing to comply with a collection of information if it does not display a currently valid OMB control number.

1. REPORT DATE <b>26 JUL 2006</b>	2. REPORT TYPE <b>Final Report (Technical)</b>	3. DATES COVERED <b>03-06-2005 to 03-12-2005</b>	
4. TITLE AND SUBTITLE <b>Study on PCB Properties of Epoxy Based Nanocomposites with Different Types of Layered Hybrid Materials</b>		5a. CONTRACT NUMBER <b>FA520905P0494</b>	
		5b. GRANT NUMBER	
		5c. PROGRAM ELEMENT NUMBER	
6. AUTHOR(S) <b>Tsung-Yen Tsai</b>		5d. PROJECT NUMBER	
		5e. TASK NUMBER	
		5f. WORK UNIT NUMBER	
7. PERFORMING ORGANIZATION NAME(S) AND ADDRESS(ES) <b>Chung Yuan Christian University, 200 Chung Bay Road, Chung-Li 32023, Taiwan, NA, 32023</b>		8. PERFORMING ORGANIZATION REPORT NUMBER <b>AOARD-054062</b>	
9. SPONSORING/MONITORING AGENCY NAME(S) AND ADDRESS(ES) <b>The US Resarch Labolatory, AOARD/AFOSR, Unit 45002, APO, AP, 96337-5002</b>		10. SPONSOR/MONITOR'S ACRONYM(S) <b>AOARD/AFOSR</b>	
		11. SPONSOR/MONITOR'S REPORT NUMBER(S) <b>AOARD-054062</b>	
12. DISTRIBUTION/AVAILABILITY STATEMENT <b>Approved for public release; distribution unlimited</b>			
13. SUPPLEMENTARY NOTES			
14. ABSTRACT <b>The contractor shall investigate: (1) An epoxy/clay nanocomposite matrix material for printed circuit boards, (2) A prepreg for printed circuit boards which contains the epoxy/clay nanocomposite matrix material, and (3) A printed circuit board made with at least one of proposed prepregs.</b>			
15. SUBJECT TERMS <b>Polymer/Clay Nanocomposite Materials, Holographic Materials, Inorganic/Organic Materials</b>			
16. SECURITY CLASSIFICATION OF:			17. LIMITATION OF ABSTRACT
a. REPORT <b>unclassified</b>	b. ABSTRACT <b>unclassified</b>	c. THIS PAGE <b>unclassified</b>	
			18. NUMBER OF PAGES <b>22</b>
19a. NAME OF RESPONSIBLE PERSON			

## Progress Report –

### Proposal abstract

Development of fabrication process to realize nearly intrinsic GaAs-based NEMS mechanical resonator is proposed. The development of GaAs-based NEMS mechanical resonator will allow for systematic study of intrinsic energy-loss mechanisms in NEMS resonators. Which full understanding will allow for the development of more sensitive NEMS devices. For such endeavor, a hetero-epitaxy system with near perfect lattice match as well as a near perfect selective etch chemistries – GaAs/InGaP – will be characterized. Along with GaAs-based NEMS development, DMS-based spin-diode devices will be fabricated and characterized.



### Report Summary

We developed a fabrication method to realize GaAs nanomechanical resonators without a plasma process. Avoiding plasma processing, we were able to realize GaAs NEMS resonators of high Q factors, comparable to Si NEMS resonators of similar size. Such realization was made possible by utilizing latticed matched GaAs/InGaP heterostructures allowing for near perfect selective etch chemistries. The processing and measurement techniques are detailed in Appendix I & II.

### Publications –

Two manuscripts under preparation & S.B. Shim, S.W. Kang, J.H. Kong, K. Char, and Y.D. Park, *Development of plasma-free etch chemistry to realize defect-free GaAs micromechanical resonator structures*, Institute of Physics Conference Series: Compound Semiconductors 2004 184, 349 (2005).

### Presentations –

- “The energy dissipation from Joule heating in GaAs nanomechanical resonator” MRS Spring Symposium, 4/20/2005.
- “Development of GaAs based NEMS processing for investigation of energy loss mechanisms in resonators” 2<sup>nd</sup> US-Korea Workshop on Nanoelectronics & 4<sup>th</sup> US-Kore Workshop on Nanostructures Materials and Manufacturing, KIST, 4/25/2005
- “Effect of Induced Strain on GaAs Nanomechanical Resonator” APS March Meeting, 3/24/2005

**APPENDIX I:** The following is summary of the following publication (with funding source properly acknowledged):

S.B. Shim, S.W. Kang, J.H. Kong, K. Char, and Y.D. Park, *Development of plasma-free etch chemistry to realize defect-free GaAs micromechanical resonator structures*, Institute of Physics Conference Series: Compound Semiconductors 2004 184, 349 (2005).

## **Development of plasma-free etch chemistry to realize defect-free GaAs micromechanical resonator structures**

### **1. Introduction**

Micro-electromechanical systems (MEMS) are of high commercial and scientific interest as promises of micrometer-sized sensors and actuators are being realized in such diverse areas as automotive to bio-technology to defense industry/applications. Recently, mechanical functionality at the nanometer-sized scale has received considerable attention, as nano-electromechanical system (NEMS) sensors function at higher fundamental frequencies allowing for highly sensitive force measurements. A successful development of NEMS based devices promises to expand our physical understanding of forces at the smallest dimensions to atomic force microscopy-based memory elements. Along with promises of functional applicable devices, NEMS systems allow for fundamental insights into science [1].

### **2. GaAs-based micromechanical resonators**

Although Si-based MEMS and NEMS structures have a firm standing, compound semiconductor based, especially, GaAs-based NEMS structures offer unique properties advantageous for NEMS development. Recently, Knobel and Cleland demonstrated nanometer-scale displacement sensing using GaAs-based NEMS resonator – in efforts to observe quantum mechanical effects on *macroscopic* mechanical oscillator [2]. Their detection scheme utilized the piezoelectric properties of GaAs which signal was coupled to a single-electron transistor [3]. A reason for such conditioning of displacement signal is the fact that the Q (quality) factor has been found to scale with volume of the resonator. Energy dissipation,  $Q^{-1}$ , is known to be more problematic as dimensions are reduced. Particularly, GaAs-based resonators are generally fabricated from GaAs/AlGaAs heterostructures. To increase selectivity between GaAs and AlGaAs (typically HF wet etch chemistries), higher Al content is required, introducing greater strain in the GaAs resonator. GaAs are also typically defined by chemical reactive ion etch methods, possibly introducing damage as well as impurities into the GaAs resonator structure.

### **3. GaAs/InGaP**

#### *3.1. Microresonator structures*

GaAs micromechanical resonator structures were realized utilizing plasma-free etch chemistry, by utilizing nearly latticed-matched GaAs/In<sub>0.5</sub>Ga<sub>0.5</sub>P alloy system patterned by selective wet-etch chemistries. Unintentionally doped GaAs (500 nm)/InGaP(500 nm) epilayers were grown on semi-insulating GaAs (001) substrates by low pressure metal-organic chemical vapor deposition (LP-MOCVD). GaAs cap layer was defined with photoresists and patterned in a citric acid/hydrogen peroxide solution, resulting in near vertical side-wall profiles with high selectivity of GaAs over InGaP. After GaAs cap patterning and resist removal, hydrogen chloride

solutions of varying concentrations were investigated for selectivity of InGaP over GaAs at varying etch temperatures, with agitation conditions, and for differing crystallographic directions.

HCl was found to possess near perfect selectivity of InGaP over GaAs. For 12 M HCl solution, vertical etch-rate was found to be nearly  $3 \mu\text{m}/\text{minute}$  under agitation. As the GaAs substrate acts as an etch stop, lateral etch of InGaP layer between GaAs layers starts with initial etch fronts of vee, mixed, and dovetail observed by cross-sectional scanning electron microscopy with predominance of dovetail etch front for lateral etch direction  $45^\circ$  from the cleave direction (Figure 1). The lateral etch rate at room temperature for 12 M HCl solution was highly directional dependent with GaAs cap edge patterned parallel to the cleave direction [011] of nearly zero lateral etch rate and edge  $45^\circ$  from the cleave direction to be nearly  $1 \mu\text{m}/\text{min}$ , similar behavior as observed by Cich *et al.* [4]. For increasing dilution of HCl, the etch rate, especially lateral etch rate, was drastically reduced, with no observable lateral etch at 1:4 HCl:H<sub>2</sub>O. Typically, etch rate was found to be agitation independent. Realization of suspended GaAs resonator structures with aspect ratios as high as 30 was achieved by simply drying in a flow of dry Nitrogen gas.

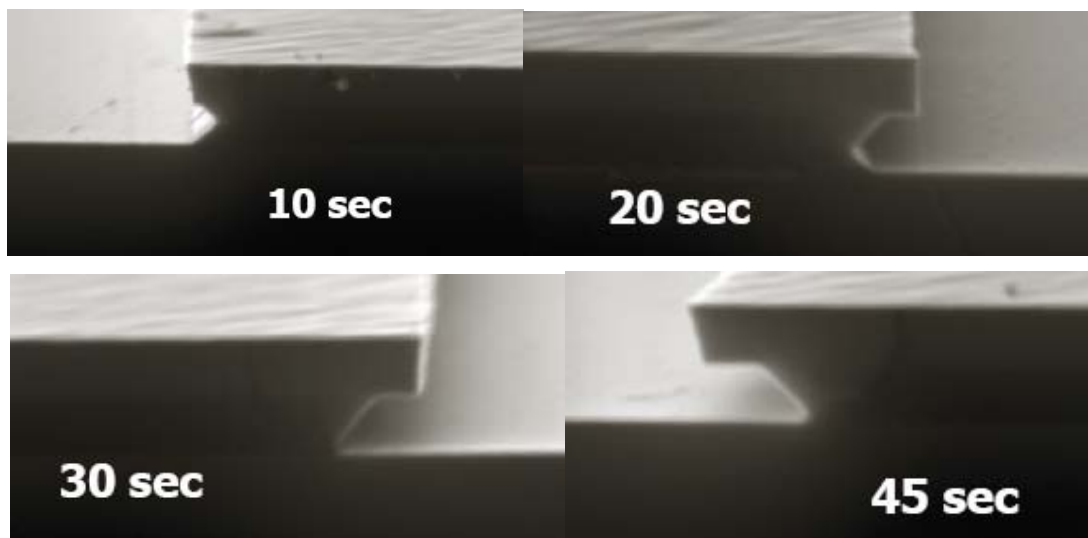


**Figure 1** – Evolution of InGaP etch front in 12M HCl solution. Top layer is 500 nm thick GaAs. InGaP layer is 500 nm thick on GaAs (001) substrate.

### 3.2. Nanoresonator structures

To realize submicrometer-sized resonator structures, electron-beam lithography (EBL) techniques were utilized to pattern etch-mask (typically Au/Ti) from subsequent e-beam evaporation and lift-off. It was found that although the commercially available PMMA EBL resist although showed no marked deterioration during the etch process, etching process through a masked opening was found to lower the etch rate indeterminately. Thus, Au/Ti was e-beam evaporated to be used as an etch mask for subsequent processing. Au/Cr did not bid well as an etch mask as the underlying Cr layer was found to be etched during the HCl InGaP removal. Utilizing e-beam lithography, we were able to realize both beam resonator structures with length to width ratios as high as 40 and torsional resonator structures.

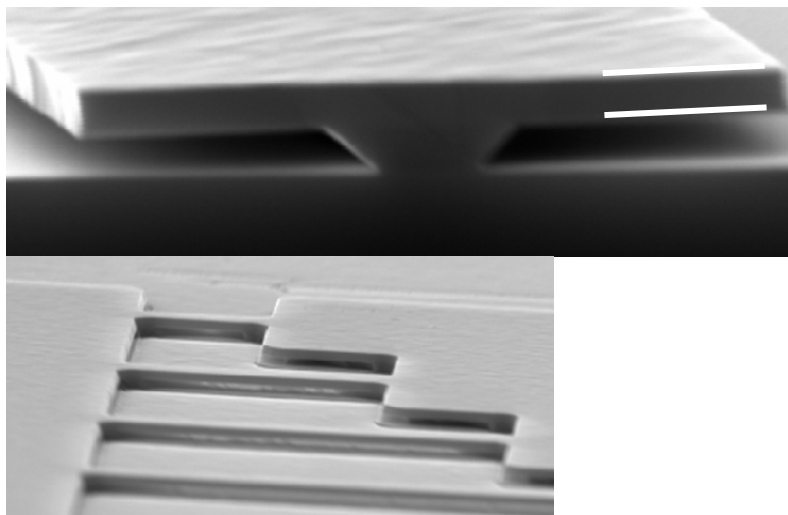


**Figure 2** – Cross-sectional SEM micrograph of under 500 nm GaAs suspended by etched InGaP layer (above) and resulting GaAs resonator structures (2  $\mu\text{m}$  wide) of varying lengths (and aspect ratios).

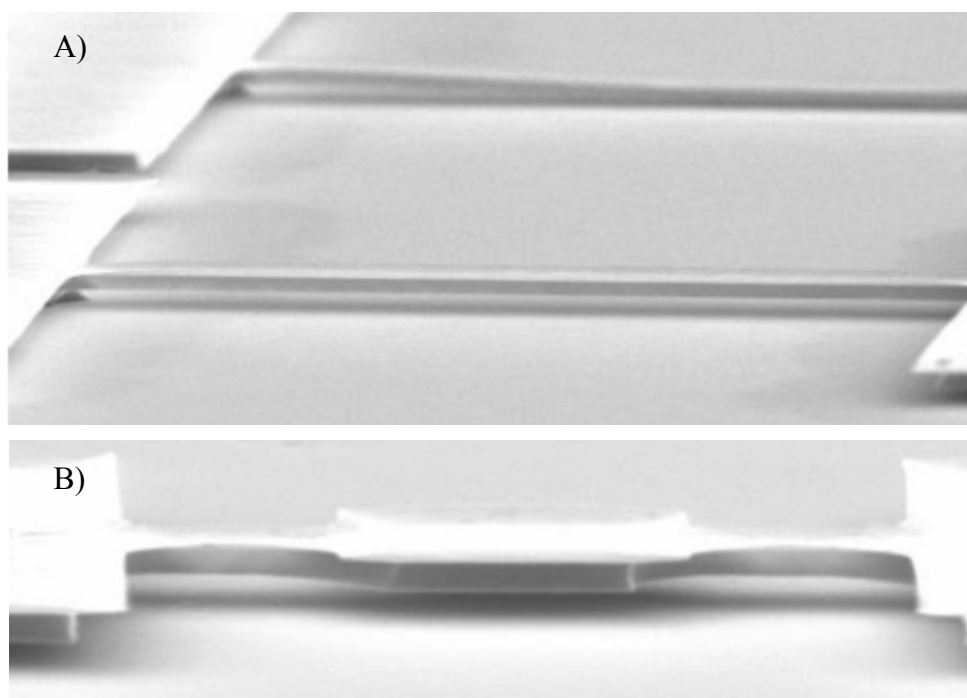


**Figure 3** – 500 nm thick GaAs epilayer is patterned to realize a) beam resonator structure with width of 400 nm and length of 28 microns (in foreground, the structure in the background is a higher aspect ratio test structure); and b) torsional resonator structure of inner 3 x 3  $\mu\text{m}^2$  ‘paddle.’ For both cases, EBL followed by e-beam evaporation of Ti/Au were used before standard etch of GaAs and InGaP.

#### **4. Summary**

Two different resonator structures have been fabricated by plasma-free chemistry process. Citric acid based etch was found to be near perfectly selective of GaAs over InGaP. Concentrated HCl etch was found to be perfectly selective of InGaP over GaAs. Both etch chemistries were found to be compatible with standard photolithography and electron-beam lithography processing, although for GaAs etch, the etch rate was indeterministically slowed through a resist opening. Using EBL, aspect ratios as high as 40 were realized along with 3 micron x 3 micron torsional resonator structures suspended by sub-micron mechanical supports.

This work has been supported by KOSEF through CSCMR, by KIST Vision21 Spintronics Project, and by US Army Research Laboratory through the Office of Naval Research (ONR N62649-03-1-0010) Far East Program.

#### **References**

- [1] LaHaye M D et al. 2004 Science 304 74 -77
- [2] Knobel R G and Cleland A N 2003 Nature (London) 424 291-293
- [3] Knobel R G and Cleland A N 2002 Applied Physics Letters 81 2258-2260
- [4] Cich M J et al. 2003 Applied Physics Letters 82 651-653

**APPENDIX II:** The following is preview summary of a manuscript describing the resulting characterization of GaAs resonators:

S.B. Shim, S.W. Kang, Y.D. Park, A. Gaidarzhy, and P. Mohanty, to be submitted.

## 1. Introduction

The researches in nanoelectromechanical system (NEMS) are being developed aggressively for widening its application capabilities and for opening new regime toward quantum mechanics. The application possibilities are such as high frequency filters [1, 2], ultra sensitive mass sensors which have  $10^{-18}$ g resolution [3, 4], ultrafast actuators [5] and memory elements using the nonlinear properties of the system [6, 7]. And the studies of NEMS at ultra low temperature give us possibility to realize and observe quantum system either by attaching small cantilever on the central beam [8] or by designing ultrasensitive circuit to detect the motion close to quantum limit [9].

Inside of these researches, there is another desire which is realizing low energy loss system and high quality factor mechanical system. Conventionally, the quality factor of mechanical resonator decreases when the dimension decreases [10, 11, 12]. The resonator with mm range size gave us  $10^5 \sim 10^6$  quality factor [13]. But in micrometer size, usual resonator has  $10^3 \sim 10^4$  quality factor [14, 15]. These values even get lower in GaAs based mechanical resonators. So, to realize low energy dissipative system with GaAs, we need to eliminate any possible source of energy dissipation of the system.

Previous study in GaAs based MEMS and NEMS, GaAs/AlGaAs heterostructure were used [16, 17, 18]. To fabricate sample with this structure, we need to increase the Aluminum contents up to 70% to increase the selectivity between GaAs and AlGaAs [19]. And it gives internal strain on the device layer which can be a source of energy dissipation due to the dislocation in the interface. In addition to that, the conventional fabrication process has RIE step for GaAs layer etching. It has an advantage of side wall profile in the device but at the same time, we introduce plasma damage in the device layer which is an important source of energy dissipation.

We solved these problems by using lattice matched GaAs/ $\text{In}_{0.481}\text{Ga}_{0.519}\text{P}$  heterostructure with plasma free etch technique. We can minimize the internal strain because GaAs/InGaP hterostructure is lattice matched structure. Additionally, GaAs and InGaP have perfect etch chemistry (Citric Acid and Hydrochloric acid) which minimize the fabrication damage due to plasma process. In the next section, we will describe the realization of nanomechanical resonator with plasma free etch technique.

## 2. Experiment

The lattice matched GaAs/InGaP heterostructure was grown epitaxially by Metal Oxide Chemical Vapor Deposition (MOCVD) on semi-insulate GaAs substrate. 500nm thick InGaP sacrificial layer was grown on (100) GaAs substrate and 500nm thick GaAs device layer was grown on top of InGaP layer.

Standard electron beam lithography technique was used to define the structure on the sample. The focused electron beam of scanning electron microscope was controlled by vector utilized beam control system. Followed by development, 50nm of Au and 5nm Ti adhesion layer were evaporated to define the beam, electrically connect the structure and act as an etch mask for the following etching processes.

In previous study, the device layer which is GaAs was usually etched by Chlorine based RIE process. By using RIE with proper ratio of reactive gas, we can

get nice side wall profile for the device. But, during the process, plasma damage is inevitably introduced on the device layer [20, 21]. And the plasma induced damage can make dislocations in the device layer and as a result of these dislocations the Q-factor of the system decreases. As a possible solution of reduce dislocation and realization of high Q system, we adopted plasma free etch technique with the mixture of Citric acid and Hydrogen peroxide [22]. Usually, chemical etching is isotropic. But, GaAs has strong crystallographic dependence in chemical etching process [23]. So, by rotating the pattern on the device layer, we can get good side wall profile for the device. Figure 1 shows the side wall profiles according to the orientation of pattern. The side face of (c) which the pattern is parallel to (110) direction shows the highest anisotropic nature. And this direction matches to the fastest etching direction of sacrificial InGaP layer.

The removal of sacrificial InGaP layer is important to realize suspended structure. First of all, the etching process needs to be isotropic for the removal of InGaP right underneath of GaAs device layer. And the selectivity for the device layer and sacrificial layer should be high otherwise the device layer can be etched in the course of sacrificial layer etching. For these, we have selected HCl to etch the InGaP layer. By this choice, we get the selectivity which is higher than 100.

We determined the selectivity by investigation the etch rate of each layers. In 12M HCl solution, vertical etch rate of InGaP layer is about 1 $\mu$ m/min and it doesn't have any directional dependence. But the lateral etching is different. Lateral etching has strong dependence on the crystallographic orientation of InGaP layer face to the chemical because of the reaction speed between InGaP and HCl [24]. So, we rotated the direction of the beam parallel to (100) direction to increase the etch rate to same rate with vertical. Figure 3 (a) shows the SEM micrograph of the resonator and the beam has 15 $\mu$ m length and 500nm width and 500nm thickness.

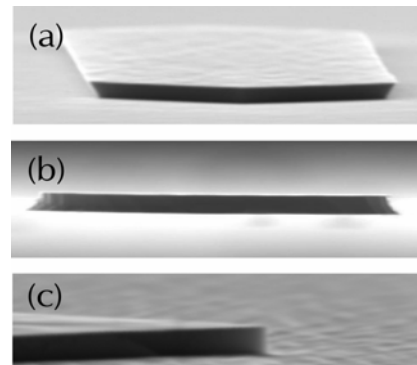


Figure 1. Various side wall profiles of GaAs layer which are etched by Citric Acid/H<sub>2</sub>O<sub>2</sub>. The pattern orientations are (a) (0-11), (b) (011) and (c) (100)

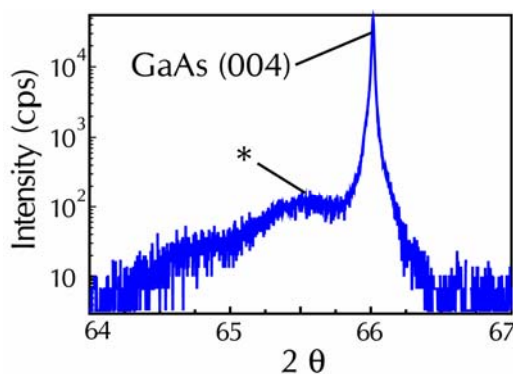


Figure 2.  $\theta$ - $2\theta$  X-ray diffraction scans was performed using Cu K $\alpha$  radiation. Clear diffraction peak was observed at 66 degree same for both GaAs and InGaP. The broad peak at 65.5 degree shows the weak strain caused by small lattice mismatch from growth.

We started the characterization from High Resolution X-Ray Diffraction (HRXRD) to check the lattice is matched or not. As we mentioned before, GaAs/InGaP heterostructure is lattice matched structure. So, we can only observe GaAs (004) peak which means the lattice constant is close enough (Figure 3). So HRXRD can't recognize the difference of the lattice constant between two layers. But in Figure 2, we can see broad peak around  $65.5^\circ$ . This means the lattice constant of InGaP layer is slightly larger so the relaxed lattice constant shows that broad peak. This broad peak appears because of the size difference of the ions. The size of In ion (0.081nm) is bigger than Ga (0.062nm) so when we replace Ga with In, the lattice constant is slightly increase. With these result, we can say that the lattice of the two layers are matched well there is almost no internal stress on the GaAs layer which is good for reducing the energy dissipation.

The GaAs mechanical resonator was characterized with standard magnetomotive technique [25, 26]. We placed the resonator inside of  $^3\text{He}$  refrigerator (260mK base temperature) with high vacuum ( $10^{-6}$  Torr). The long axis of the resonator was located perpendicular to a magnetic field generated by 9T superconducting magnet. Network Analyzer generated alternating current along the length of the resonator and measured the response of the beam. The alternating current which is perpendicular to the magnetic field generates a Lorentz force that makes oscillatory motion of the beam. Then, the resulting oscillatory motion of the beam is

$x(\omega) = F_{dr}(\omega) / [(\omega_0^2 - \omega^2 + i\omega\omega_0/Q)m]$  and this displacement  $x$  in the magnetic field  $B$  induces  $V_{emf}(\omega) = \xi LB\omega_0 x(\omega)$  in the Au electrode. Here the constant  $\xi$  is a mode-dependent integration constant [27]. And the  $V_{emf}$  is detected by network analyzer. Figure 3 (a) shows schematic diagram of measurement setup.

### 3. Results and discussion

The mechanical resonance frequency for a doubly clamped beam is given by  $f_0 \propto \sqrt{\frac{E}{\rho}} \frac{w}{L^2}$  where  $E$  is Young's modulus,  $\rho$  is the density,  $w$  is the width of the beam along the direction of motion and  $L$  is the beam length. The measured resonant frequency of the beam is 17.973MHz with 11,000 quality factor. Figure 3 (b) shows Lorentzian shape of the amplitude which is calculated from magnetomotive relation

$$V_{emf}(\omega) = \frac{i\omega\xi L^2 B^2 / m}{\omega_0^2 - \omega^2 + i\omega\omega_0 / Q} I_{dr}(\omega) \quad (1)$$

And figure 3 (c) shows the phase shape corresponds to the amplitude.

This quality factor 11,000 is the highest value in GaAs based mechanical resonator at submicron size. In GaAs based MEMS and NEMS studies, the reported quality factor is order of  $10^3$  with sub-micrometer dimension [16, 17, 18]. Our result is one order higher than previous result at these dimensions. There can be several

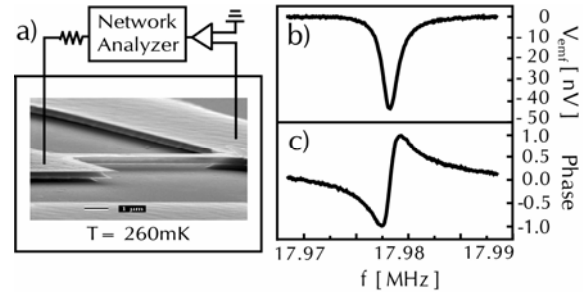


Figure 3. a) SEM micrograph of the 15  $\mu\text{m}$  nanobeam. The diagram shows the measurement circuit. b) The fundamental resonance mode of the beam is at 17.983 MHz with Q of 11,000. The induced  $V_{emf}$  is a Lorentzian peak after

interpretation of this result. First of all, conventional fabrication method includes RIE process for etching of device layer. As I mentioned before, the plasma can induce unintended fabrication damage and it gives dislocation on the device layer. And this dislocation is a source of energy dissipation [10]. Secondly, most of previous researches used GaAs/AlGaAs heterostructure which has some disorder in the interface also can be a source of energy dissipation. In this report, by using lattice matched GaAs/InGaP heterostructure and plasma free etch chemistry, we can realize high quality factor mechanical resonator.

We also have measured the response of resonator with different driving power. During this measurement, the temperature was held at 260mK and the applied magnetic field was 4T. The resonant peak grew linearly in log scale. And the response shows nonlinearity at high driving power [Figure 4 (a)]. Figure 4 (b) is the plot of amplitude as a function of driving power. By the equation (1), the amplitude is proportional to the driving current. We also convert the amplitude value to driving force with  $F_{dr} = I(\omega)B$ . And the center beam displacement is given by  $\Delta x = \frac{V_{emf}}{\xi BL\omega}$ , so we

can calculate the effective spring constant of the beam. The calculated effective spring constant,  $k_{eff} = QF_{dr}(\omega_0) / \Delta x$  of GaAs nano-beam is  $k_{eff} = 13,200 N / m$ . [Figure 4 (b)]

According to the magnetomotive relation, the  $V_{emf}$  has quadratic dependence on the applied magnetic field. Near the resonance, equation (1)

becomes  $V_{emf} = \frac{\xi LL_{beam} B^2 \omega_0}{k} Q I_{dr}(\omega)$  where  $\omega_0 = \sqrt{\frac{k}{m}}$ . The response of the beam satisfies

this relation as shown in Figure 4 (c). And the field dependence of energy dissipation is also shows quadratic dependence. [Figure 4 (d)]

We measured the resonant peak shift and the dissipation as a function of temperature. These are the real and imaginary parts of the susceptibility  $\chi = \chi' + i\chi'' \cong \rho v^2 (2\delta f / f_0 + iQ^{-1})$  [28]. In Figure 5, we can see the logarithmic temperature dependence in frequency shift data. The resonant peak shows weak degradation when the temperature is increased. And we can see the saturation of the frequency shift below 500mK. The energy dissipation shows very weak power law where 0.07 is the power. And it also shows the saturation below 500mK. In previous research, the

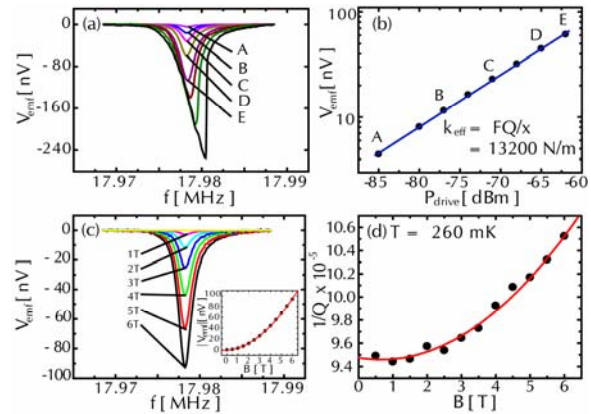


Figure 4. a) The change of resonance peak as a function of driving power. The peak is Lorentzian in the linear regime and the shape shows asymmetric nonlinear shape when the driving power is higher than -60dBm. b) Linear dependence of amplitude as a function of driving power at 4 Tesla magnetic field. The amplitude corresponds to the displacement of the beam  $x$ , and the driving power corresponds to the driving force. The calculated effective spring constant is 13,200N/m. c) The response of the oscillator shows quadratic dependence on applied magnetic field  $B$ . d) The energy dissipation as a function of applied magnetic field.

energy dissipation due to two level system is proportional to  $T$  or  $T^3$  [28]. But the power dependence of this result is much weaker than it. This means our GaAs resonator has less damage or dislocation on the device layer so the energy dissipation shows weak dependence on the temperature.

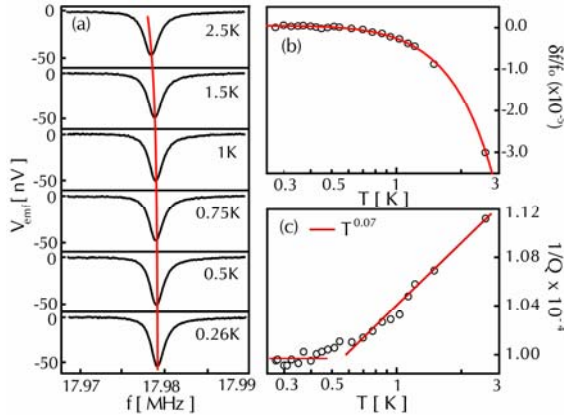


Figure 5. a) The change of resonance peak as temperature is changed. b) Corresponding frequency shift  $\delta f/f_0$  as a function of temperature. c) Energy dissipation when the temperature is increased. The dissipation shows weak power law dependence  $T^{0.07}$ .

#### 4. Conclusion

We have fabricated doubly clamped nanomechanical resonator from GaAs/InGaP lattice-matched heterostructure by utilizing plasma free etch technique. The perfect selective etch chemistries for GaAs and InGaP enable us fabrication easier. Owing to this plasma free etch technique, we can reduce the fabrication damage on the device layer. We characterized the GaAs mechanical resonator with standard magnetomotive technique at low temperature (260mK) with 6T magnetic field. The resonance was shown at 17.98MHz with high quality factor 11,000. Plasma free etch technique gives us the increasing of quality factor because there is no plasma induced dislocation in the device layer. And energy dissipation measurement shows weak dependence on the temperature. In summary, we realized and characterized defect free mechanical resonator from GaAs/InGaP heterostructure. And this resonator has record high quality factor in GaAs based mechanical resonator at sub-micrometer dimension.

#### References

- [1] J.F. Rhoads, S.W. Shaw, K.L. Turner and R. Baskaran, *J. Vib. Acoust.*, **125**, 423 (2005)
- [2] T. Kemp and M. Ward, *Sensors and Actuators A*, **123-124**, 281 (2005)
- [3] K.L. Ekinci, X.M.H. Huang, and M.L. Roukes, *Appl. Phys. Lett.* **84**, 4469 (2004)
- [4] K.L. Ekinci, Y.T. Yang and M.L. Roukes, *J. Appl. Phys.* **95**, 2682 (2004)
- [5] X.T. Wu, J. Hui, M. Young, P. Kayatta, J. Wong, D. Kenneth, J. Zhe and C. Warde, *Appl. Phys. Lett.*, **84**, 4418 (2004)
- [6] R.L. Badzey and P. Mohanty, *Nature*, **437**, 995 (2005)
- [7] R.L. Badzey, G. Zolfagharkhani, A. Gaidarzhy and P. Mohanty, *Appl. Phys. Lett.*, **85**, 3587 (2004)
- [8] A. Gaidarzhy, G. Zolfagharkhani, R.L. Badzey and P. Mohanty, *Phys. Rev. Lett.*, **94**, 030402 (2005)
- [9] M.D. Lahaye, O. Buu, B. Camarota and K.C. Schwab, *Science*, **304**, 74 (2004)
- [10] P. Mohanty, D.A. Harrington, K.L. Ekinci, Y.T. Yang, M.J. Murphy and M.L. Roukes, *Phys. Rev. B*, **66**, 085416 (2002)

- [11] D.W. Carr, S. Evoy, L. Sekaric, H.G. Craighead and J.M. Parpia, *Appl. Phys. Lett.*, **75**, 920 (1999)
- [12] R.E. Mihailovich and N.C. MacDonald, *Sensors and Actuators A*, **50**, 199 (1995)
- [13] R.A. Buser and N.F. de Rooij, *Sensors and Actuators A*, **21-23**, 323 (1990)
- [14] A.N. Cleland and M.L. Roukes, *Appl. Phys. Lett.*, **69**, 2653 (1996)
- [15] D.W. Carr and H.G. Craighead, *J. Vac. Sci. Technol. B*, **15**, 2760 (1997)
- [16] H.X. Tang, X.M.H. Huang, M.L. Roukes, M. Bichler and W. Wegscheider, *Appl. Phys. Lett.*, **81**, 3879 (2002)
- [17] R. Knobel and A.N. Cleland, *Appl. Phys. Lett.*, **81**, 2258 (2002)
- [18] A.N. Cleland, J.S. Aldridge, D.C. Driscoll and A.C. Gossard, *Appl. Phys. Lett.*, **81**, 1699 (2002)
- [19]
- [20] S.W. Pang, D.D. Rathman, D.J. Silversmith, R.W. Mountain and P.D. DeGraff, *J. Appl. Phys.*, **54**, 3272 (1983)
- [21] S.W. Pang, G.A. Lincoln, R.W. McClelland, P.D. DeGraff and M.W. Geis, *J. Vac. Sci. Technol. B*, **1**, 1334 (1983)
- [22] A.R. Clawson, *Materials Science and Engineering R*, **31**, 1-431 (2001)
- [23] R.P. Ribas, Maskless front-side bulk micromachining to standard GaAs IC technology.
- [24] M.J. Cich, J.A. Johnson, G.M. Peake and O.B. Spahn, *Appl. Phys. Lett.*, **82**, 651 (2003)
- [25] D.S. Greywall, B. Yurke, P.A. Busch, A.N. Pargellis and R.L. Willett, *Phys. Rev. Lett.*, **72**, 2992 (1994)
- [26] A.N. Cleland and M.L. Roukes, *Sensors and Actuators*, **72**, 256 (1999)
- [27] R.G. Knobel and A.N. Cleland, *Nature*, **424**, 291 (2003)
- [28] G. Zolfagharkhani, A. Gaidarzhy, S.B. Shim, R.L. Badzey and P. Mohanty, in press